Article:
Wang, Wei, Zhang, Xiaoqian, Xu, Huanfeng et al. (4 more authors) (2018) Evidence for Layered Quantized Transport in Dirac Semimetal ZrTe5. Scientific Reports. 23011. ISSN 2045-2322

https://doi.org/10.1038/s41598-018-23011-3

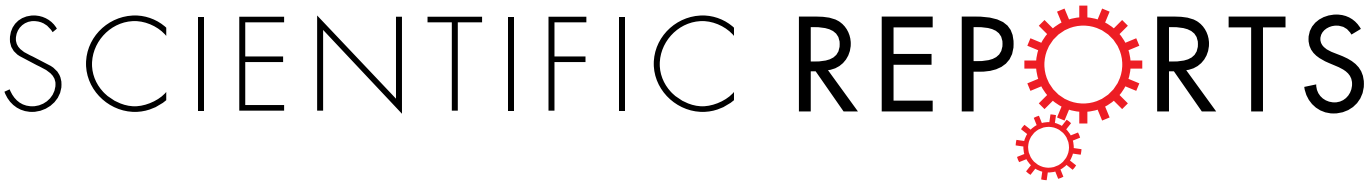

OPEN

Evidence for Layered Quantized Transport in Dirac Semimetal $ZrTe_5$

Wei Wang[1], Xiaoqian Zhang[1], Huanfeng Xu[1], Yafei Zhao[1], Wenqin Zou[1], Liang He[1] & Yongbing Xu[1,2]

Received: 20 September 2017
Accepted: 22 February 2018
Published online: 23 March 2018

$ZrTe_5$ is an important semiconductor thermoelectric material and a candidate topological insulator. Here we report the observation of Shubnikov-de Hass (SdH) oscillations accompanied by quantized Hall resistance in bulk $ZrTe_5$ crystal, with a mobility of 41,000 $cm^2V^{-1}s^{-1}$. We have found that the quantum oscillations does not originate from the surface states, but from the bulk states. Each single layer $ZrTe_5$ acted like an independent 2D electron system in the quantum Hall regime having the same carrier density and mobilities, while the bulk of the sample exhibits a multilayered quantum Hall effect.

The layered $ZrTe_5$ crystal, with large thermopower[1–5], has been studied by scientists for many years. Recently, it has attracted more attention after been predicted as a 2D topological insulator(TI) with a bulk direct band gap of 0.4 eV[6]. But experimentally, the topological nature of $ZrTe_5$ is still under debate. Some studies reported $ZrTe_5$ as a weak TI[7,8]. While, several other experimental studies have suggested that $ZrTe_5$ might be a Dirac semimetal[9,10]. The discrepancy may come from the fact that $ZrTe_5$ is in a topological critical state placed between a weak-TI and a strong-TI which is sensitive to the lattice constant. The lattice constant is influenced by the growth conditions and the measurement environments.

In this work, we have studied the quantum oscillations of bulk $ZrTe_5$ grown by the chemical vapor transport method (CVT) using iodine as the transport agent. Quantum oscillations from the bulk states have been observed having a high mobility of 41000 $cm^2V^{-1}s^{-1}$. The Fermi surface was shown to be two-dimensional with a Berry phase of π in the infinite field limit, which indicated that $ZrTe_5$ is a topologically non-trivial material. More importantly, we have found quantized Hall resistance with a filling number of $\nu = n + 1/2$, and quantized step size of ~e^2/h per monolayer. Both SdH oscillations and quantized Hall resistance suggest that $ZrTe_5$ is a 2D non-trivial material with weak inter-layer interactions.

Results

Electronic structure of $ZrTe_5$. As shown in Fig. 1a, the structure of the transition-metal Pentatelluride $ZrTe_5$ exhibits a quasi-two-dimensional structure (space group is *Cmcm*). Within the *a*-*c* plane, zigzag chains of Te atoms along the *a*-axis are linked to trigonal prismatic chains of $ZrTe_3$ running along the *c*-axis. The 2D planes bond weakly via van der Waals forces along the *b*-axis, forming the 3D bulk crystal.

To verify the band structure of $ZrTe_5$ crystal, we performed angle-resolved photoemission spectroscopy (ARPES) measurements, using a photon energy of 21.2 eV (He I α resonance line). Figure 1c shows the electron E-K diagram around the center of the Brillouin zone (Fig. 1b). Near the Γ point, we measured a linear E-K dispersion (as indicated by the red dashed lines in Fig. 1c), suggesting the presence of Dirac fermions. At the Γ point, the Fermi level is very close to the top of the valence band at 300 K, which implies a hole dominated electronic structure, consistent with previous transport measurement work[10].

Temperature-dependence of the longitudinal resistivity of $ZrTe_5$ crystal. Figure 2a shows the longitudinal resistivity as a function of temperature for the $ZrTe_5$ sample. At room temperature, the resistivity is ~0.7 mΩ·cm, suggesting a poor semimetal. As the temperature decreases from 300 K, the resistivity increases exponentially like that of a semiconductor. The activation energy can be estimated from the Arrhenius plot of $\ln(\rho_{xx})$ vs $1/T$ for high temperatures, as shown in Fig. 2a (right inset). We measure an activation energy of 41 meV, which is close to the Fermi level position in the work by Shaochun Li *et al.*'s result[7]. At $T = 140$ K, the resistivity reaches a maximum. This is also accompanied with the changing of carriers from hole-dominated to electron-dominated as the temperature decreases.

[1]National Laboratory of Solid State Microstructures, School of Electronic Science and Engineering and Collaborative Innovation Center of Advanced Microstructures, Nanjing University, Nanjing, 210093, China. [2]Department of Electronics, York-Nanjing Joint Centre (YNJC) for spintronics and nano engineering, the University of York, York, YO10 3DD, United Kingdom. Correspondence and requests for materials should be addressed to L.H. (email: heliang@nju.edu.cn)

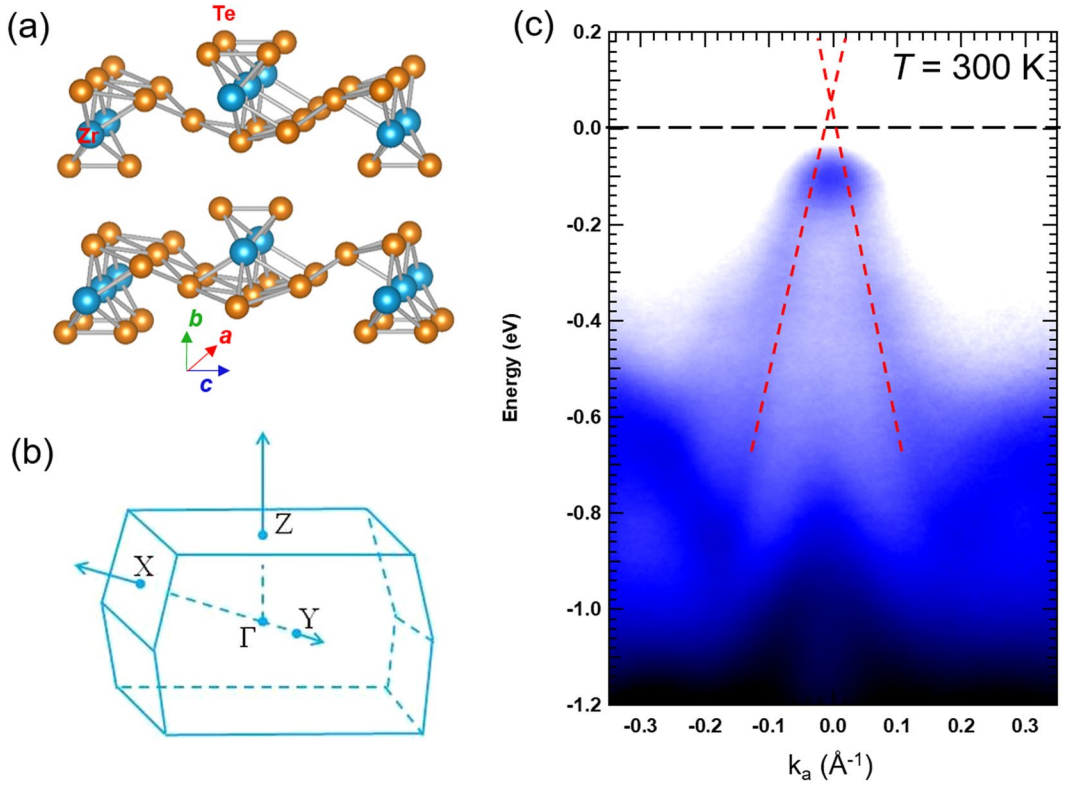

Figure 1. The electron structure of $ZrTe_5$. (**a**) Crystal structure of $ZrTe_5$. (**b**) The Brillouin zone of $ZrTe_5$. (**c**) The ARPES image of the $ZrTe_5$ at 300 K. The linear E-K relationship is indicated by red dashed lines.

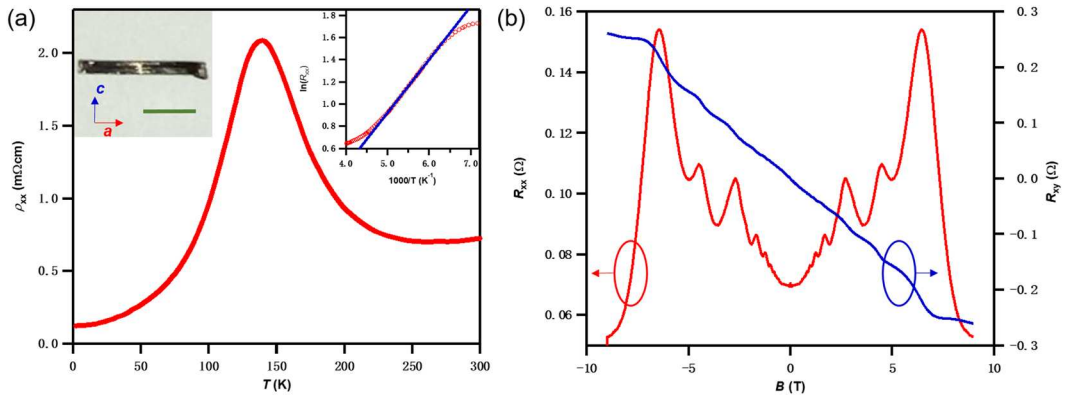

Figure 2. The R-T relationship and the magnetoresistance R_{xx} and Hall resistance R_{xy} at 2 K. (**a**) The temperature dependent resistivity of the $ZrTe_5$ sample. The current is parallel to the crystalline needle axis (I//a). Left Inset: The optic image of an as-grown bulk crystal, the scale bar is 1 mm. Right Inset: The Arrhenius plot, which yields an activation energy of 41 meV in the temperature range of 160–200 K. (**b**) The magnetoresistance R_{xx} and Hall resistance R_{xy} at 2 K. Quantum oscillations can be observed in R_{xx}, as well as plateaus in R_{xy}.

This resistivity peak, also known as the metal-insulator transition, has long been observed in various experimental reports, and the transition temperature ranges from 60 K to 145 K[9–11], depending on the detailed growth conditions. The origin of this transition has puzzled scientists for many years and the mechanism is still under debate.

Quantum oscillations in $ZrTe_5$ crystals. Figure 2b shows the longitudinal resistance R_{xx} and the Hall resistance R_{xy} as the functions of the perpendicular magnetic field (B, applied along the b-axis) at $T = 2$ K. The sample is n-type, with a carrier density $n_{3D}^{Hall} = 1.8 \times 10^{18}\,cm^{-3}$ as measured from the slope at low field. We also observe an n-p transition temperature around $T = 140$ K, which is in agreement with previous work[12]. Pronounced oscillations in R_{xx} can also be observed associated with quantized plateaus in R_{xy}. These are the quantum oscillations from the quantized Landau levels at high magnetic field. Such plateaus are very similar to

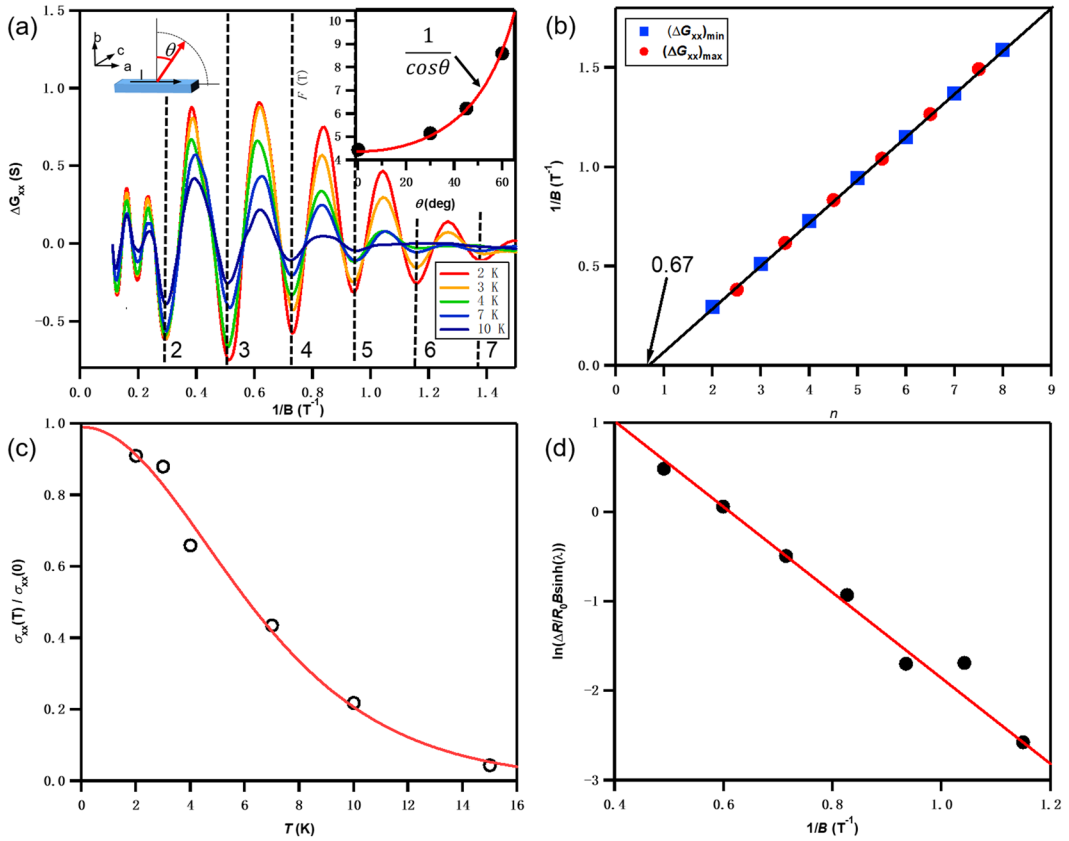

Figure 3. Quantum oscillation of $ZrTe_5$. (**a**) Shubnikov-de Hass oscillatory components at various temperatures. The oscillation frequency is ~4.6 Tesla. Right inset: The angle dependence of the oscillation frequency *f*. (**b**) Landau-level fan diagram. The linear fitting gives a nonzero intercept of 0.67, suggesting the Berry phase is close to π. (**c**) Temperature dependence of the normalized amplitude $\Delta\sigma_{xx}(T)/\Delta\sigma_{xx}(0)$. The solid red line is the best fit to $\lambda(T)/\sinh(\lambda(T))$. The magnetic field of 3.4 T was used to extract the cyclotron mass: $m_{cyc} = 0.08\ m_e$. **(d)** The Dingle plot of $\ln[(\Delta R/R_0)B\sinh(\lambda)]$ versus $1/B$ at 2 K.

the quantum Hall effect (QHE) observed in low carrier density and high mobility systems. In the $ZrTe_5$ crystal structure, the trigonal prismatic chains of $ZrTe_3$ run along the *a*-axis, forming a 2D sheet of $ZrTe_5$ in *a*-*c* plane (Fig. 1a). Because the interaction between the $ZrTe_5$ layers is weak[6], each layer $ZrTe_5$ provided an independent 2D conduction channel, as discussed later.

Here, we calculate the magnetic conductance $G_{xx} = R_{\square}/(R_{xy}^2 + R_{\square}^2)$, where $R_{\square}$ is the sheet resistance. After subtracting the non-oscillating background, the oscillatory parts of G_{xx} (ΔG_{xx}) display periodic peaks (maxima) and valleys (minima) as a function of $1/B$, where B is the magnetic field intensity. Figure 3a shows the temperature dependence of the SdH oscillations in ΔG_{xx}. The amplitudes of the oscillations decrease with increasing temperature, up to 10 K. The FFT analysis of the oscillations shows a single frequency $f = 4.6$ Tesla. The Onsager's formula gives f in terms of the cross section area of the Fermi surface (A_F) in the momentum space:

$$f = \frac{h}{4\pi^2 e} A_F \tag{1}$$

where h is the Planck constant, and e is the electron charge. For 2D carrier density: $n_{2D} = k_F^2/4\pi$. By substituting the frequency f of 4.6 Tesla, the Fermi vector k_F can be determined as 0.012 $Å^{-1}$. The 2D carrier density n_{2D} is $1.1 \times 10^{11}\ cm^{-2}$.

Figure 3a (right inset) shows the oscillation frequencies at different out-of-plane magnetic field direction θ. The $1/\cos\theta$ dependence, suggests the 2D nature of the Fermi surface.

Figure 3b shows the Landau level fan diagram. The maxima and the minima of the G_{xx} in Fig. 3a, are represented by the blue circles and red squares, respectively. The Lifshitz-Onsager quantization rule shows that $S_F\frac{\hbar}{eB} = 2\pi(n + \frac{1}{2} + \beta + \delta)$, where $2\pi\beta$ is the Berry phase and $2\pi\delta$ is the additional phase shift. For linear energy distribution Dirac fermions, the Berry phase should be π ($\beta = 1/2$). δ is determined by the dimensionality of the Fermi surface and the value changes from 0 for surface states (2D) to ±1/8 for bulk states (3D)[13]. The linear fitting of our data yields a finite intercept of 0.67 which is very close to the value of $1/2 + 1/8 = 0.625$. This result suggests a non-trivial bulk channel, that is different from strong 3D topological insulator surface states[14,15].

According to the Lifshitz-Kosevich (LK) theory[16], we can calculate the effective cyclotron mass $m_{cyc} = 0.08\ m_e$ from the temperature dependence of the SdH oscillation amplitude. The Fermi velocity is calculated as

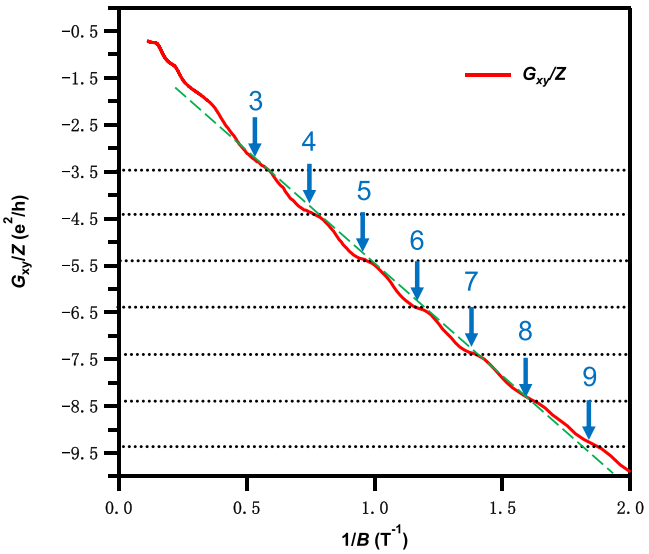

Figure 4. The bulk quantum Hall effect of $ZrTe_5$. G_{xy} divided by the number (Z) of layers plotted as a function of $1/B$, displaying quantized plateaus separated by ~1 e^2/h between adjacent LLs.

$\nu_F = \hbar k_F/m_{cyc} = 1.7 \times 10^5$ ms^{-1}, and the Fermi level $E_F = m_{cyc}\nu_F{}^2 = 13$ meV above the Dirac point, considering that electrons are the majority carrier type. Figure 3d shows the Dingle plot of $\ln[\Delta R/R_0 B\sinh(\lambda)]$ versus $1/B$. The slope is used to calculate the quantum scattering time $\tau = 1.89 \times 10^{-12}$ s. Thus the mean-free path of electrons is $l = \nu_F\tau = 3.2 \times 10^{-7}$ m, which in turn gives an estimate of the carrier mobility $\mu_{SdH} = e\tau/m_{cyc} = 41000\,cm^2V^{-1}s^{-1}$.

2D-like bulk quantum Hall effect. In Fig. 4, we plot G_{xy} divided by the number of layers (Z) in our sample as a function of $1/B$, $Z = 1.4 \times 10^5$ is calculated from the measured bulk thickness divided by the thickness of a $ZrTe_5$ monolayer. Surprisingly, the plateaus display a linear relationship with $1/B$, as indicated by the green dashed line in Fig. 4. Also, the step size between the plateaus is approximately 1 e^2/h. This suggests that the plateaus are indeed Landau levels developed under the influence of the magnetic field.

More importantly, the Landau level filling number can be indexed as $\nu = n + 1/2$, instead of n. This half-integer quantization essentially stems from the existence of the zeroth Landau level for Dirac fermions, similar to the reported bulk QHE in 3D topological insulators Bi_2Se_3[17]. This provides further evidence that $ZrTe_5$ is a topologically non-trivial material.

Discussion

According to our measurements, both the intercept of the Landau level fan diagram and the electron structure prove that the $ZrTe_5$ crystal is a topologically non-trivial material. But unlike other 3D Dirac semimetals such as Cd_2As_3, we observe that the quantum Hall plateaus in G_{xy}/Z and the step size is approximately 1 e^2/h. Similar phenomena have been observed in bulk QHE systems, like: GaAs/AlGaAs superlattice[18], Mo_4O_{11}[19] and Bechgarrd salts[20–22]. We also estimate the total carrier density as $n_{total} = n_{2D}/d = 1.1 \times 10^{11}\,cm^{-2} \times 1.38 \times 10^{17}\,cm^{-1} = 1.5 \times 10^{18}\,cm^{-3}$ (d is the thickness of monolayer $ZrTe_5$). This number is very close to the calculated Hall density of $1.8 \times 10^{18}\,cm^{-3}$. According to Hongming Weng *et al.*'s previous work[6], the $ZrTe_5$ crystal has much lower interlayer binding energy than Bi_2Se_3 and Bi(111) bilayers. That not only means the $ZrTe_5$ monolayers are easier to be exfoliated by scotch tape, but it also means that $ZrTe_5$ behaves as a series of stacked parallel 2D conduction channels. Other experiments have also shown this. For example, in Yanwen Liu *et al.*'s work, they extracted the disk-like Fermi surface of $ZrTe_5$ from the angle dependent SdH oscillations, which indicated that $ZrTe_5$ has a 2D-like band structure. In this case, we believe the QHE of our $ZrTe_5$ is due to transport through many parallel 2D conducting channels formed by the $ZrTe_5$ monolayers. Such bulk QHE was also observed in the heavily doped n-type Bi_2Se_3[17].

Thus, our analysis suggests that the inter-layer interaction of the bulk $ZrTe_5$ is relatively weak, and that $ZrTe_5$ is more likely to be a Dirac Semimetal, rather than a weak-TI.

Methods

Sample preparation. Single crystals of $ZrTe_5$ was prepared from 99.99% Zr and 99.999% Te purchased from Alfa Aesar. Single crystals were obtained by means of chemical transport reactions, using iodine as the transport agent.

Electrical measurements. The longitudinal and transvers resistance R_{xx} and R_{xy} were measured by a standard six-point Hall bar geometry in a Quantum Design physical properties measurement system (PPMS-9T). The electrical characteristics were measured using resistivity option with a current of 10 μA.

ARPES measurement. Our ARPES data were taken with a PHOIBOS 150 Hemispherical Energy Analyzer at room temperature. A He I α (21.2 eV) resonance emission line, from a high flux UVS300 He lamp was used to excite the photoelectrons from the sample surface. The UV radiation angle of incidence was 45° which relative to the sample normal and the spot size was 0.5 mm × 1 mm. All of the photoelectron measurements were performed with an angular resolution better than 0.2° in the wide-angle mode (15°) of the analyzer while the analyzer energy resolution was 30 meV.

References

1. DiSalvo, F. J., Fleming, R. M. & Waszczak, J. V. Possible phase transition in the quasi-one-dimensional materials $ZrTe_5$ or $HfTe_5$. *Physical Review B* **24**, 2935–2939 (1981).
2. Lowhorn, N. D., Tritt, T. M., Abbott, E. E. & Kolis, J. W. Enhancement of the power factor of the transition metal pentatelluride $HfTe_5$ by rare-earth doping. *Applied Physics Letters* **88**, 022101 (2006).
3. Skelton, E. *et al*. Giant resistivity and X-ray diffraction anomalies in low-dimensional $ZrTe_5$ and $HfTe_5$. *Solid State Communications* **42**, 1–3 (1982).
4. Okada, S., Sambongi, T. & Ido, M. Giant Resistivity Anomaly in $ZrTe_5$. *Journal of the Physical Society of Japan* **49**, 839–840 (1980).
5. Jackson, C., Zettl, A., Grüner, G. & DiSalvo, F. Frequency dependent conductivity in $HfTe_5$ and $ZrTe_5$. *Solid State Communications* **45**, 247–249 (1983).
6. Weng, H., Dai, X. & Fang, Z. Transition-Metal Pentatelluride ZrTe5 and HfTe5: A Paradigm for Large-Gap Quantum Spin Hall Insulators. *Physical Review X* **4**, 011002 (2014).
7. Li, X. B. *et al*. Experimental Observation of Topological Edge States at the Surface Step Edge of the Topological Insulator $ZrTe_5$. *Phys Rev Lett* **116**, 176803 (2016).
8. Wu, R. *et al*. Experimental evidence of large-gap two-dimensional topological insulator on the surface of $ZrTe_5$. *arXiv preprint arXiv:160107056* (2016).
9. Li, Q. *et al*. Chiral magnetic effect in $ZrTe_5$. *Nature Physics* **12**, 550–554 (2016).
10. Zheng, G. *et al*. Transport evidence for the three-dimensional Dirac semimetal phase in $ZrTe_5$. *Physical Review B* **93**, 115414 (2016).
11. Liu, Y. *et al*. Zeeman splitting and dynamical mass generation in Dirac semimetal $ZrTe_5$. *Nature communications* **7**, 12516 (2016).
12. McIlroy, D. N. *et al*. Observation of a semimetal–semiconductor phase transition in the intermetallic $ZrTe_5$. *Journal of Physics: Condensed Matter* **16**, L359–L365 (2004).
13. Murakawa, H. *et al*. Detection of Berry's phase in a Bulk Rashba semiconductor. *Science* **342**, 1490–1493 (2013).
14. Taskin, A. A. & Ando, Y. Berry phase of nonideal Dirac fermions in topological insulators. *Physical Review B* **84**, 035301 (2011).
15. Taskin, A. A., Ren, Z., Sasaki, S., Segawa, K. & Ando, Y. Observation of Dirac Holes and Electrons in a Topological Insulator. *Physical Review Letters* **107**, 016801 (2011).
16. Shoenberg, D. *Magnetic oscillations in metals*. Cambridge University Press (1984).
17. Cao, H. *et al*. Quantized Hall Effect and Shubnikov–de Haas Oscillations in Highly Doped Bi_2Se_3: Evidence for Layered Transport of Bulk Carriers. *Physical Review Letters* **108**, 216803 (2012).
18. Störmer, H., Eisenstein, J., Gossard, A., Wiegmann, W. & Baldwin, K. Quantization of the Hall effect in an anisotropic three-dimensional electronic system. *Physical review letters* **56**, 85 (1986).
19. Hill, S. *et al*. Bulk quantum Hall effect in $\eta-Mo_4O_{11}$. *Physical Review B* **58**, 10778 (1998).
20. Balicas, L., Kriza, G. & Williams, F. I. Sign Reversal of the Quantum Hall Number in $(TMTSF)_2PF_6$. *Phys Rev Lett* **75**, 2000–2003 (1995).
21. Cooper, J. *et al*. Quantized Hall effect and a new field-induced phase transition in the organic superconductor $(TMTSF)_2PF_6$. *Physical review letters* **63**, 1984 (1989).
22. Hannahs, S. T., Brooks, J. S., Kang, W., Chiang, L. Y. & Chaikin, P. M. Quantum Hall effect in a bulk crystal. *Phys Rev Lett* **63**, 1988–1991 (1989).

Acknowledgements

This work is supported by the National Key Research and Development Program of China (No. 2016YFA0300803), the National Basic Research Program of China (No. 2014CB921101), the National Natural Science Foundation of China (Nos. 61474061, 61674079, 11574137 and 61427812), Jiangsu NSF (BK20140054).

Author Contributions

W.W., L.H. and Y.B.X. designed the study. W.W. synthesized the $ZrTe_5$ single crystal. X.Q.Z., H.F.X., Y.F.Z. and W.W. provided ARPES measurement. W.W. and W.Q.Z. carried out low-temperature transport measurements. W.W. and L.H. wrote the manuscript. All authors discussed the results and reviewed the manuscript.

Additional Information

Competing Interests: The authors declare no competing interests.

Publisher's note: Springer Nature remains neutral with regard to jurisdictional claims in published maps and institutional affiliations.